Contrib. Astron. Obs. Skalnaté Pleso **48**, 405 – 415, (2018)

Effects of manufacturing inaccuracies on spatial resolution of lobster eye optics

V. Tichý[1], M. Barbera[2,3], G. I. Butcher[1], U. Lo Cicero[3,2], A. Collura[3], R. Hudec[4,5], A. Inneman[4], S. Varisco[3] and R. Willingale[1]

[1] *University of Leicester, Department of Physics and Astronomy, University road, LE1 7RH Leicester, United Kingdom*

[2] *Università degli Studi di Palermo, Dipartimento di Fisica e Chimica, Via Archirafi 36, 90123 Palermo, Italy*

[3] *Istituto Nazionale di Astrofisica, Osservatorio Astronomico di Palermo G.S. Vaiana, Piazza del Parlamento 1, 90134 Palermo, Italy*

[4] *Czech Technical University in Prague, Faculty of Electrical Engineering, Technická 2, 16627 Praha 6, Czech Republic*

[5] *Engelhardt Astronomical observatory, Kazan Federal University, Kremlyovskaya street 18, 420008 Kazan, Russian Federation*

Received: December 23, 2017; Accepted: March 3, 2018

Abstract. The performance of Schmidt lobster eye systems are affected by manufacturing inaccuracies in the assembly of individual mirrors or in their non ideal flatness. Such inaccuracies may significantly affect the optics performance and in particular the angular resolution. For this reason we have investigated, via ray-tracing simulations, the effects of such manufacturing inaccuracies. We report the preliminary results of this analysis and compare them with X-ray measurements performed on a test Schmidt lobster eye specimen using the 35 m long X-ray beam-line of the XACT facility of INAF-OAPA in Palermo, Italy.

Key words: lobster eye – multi-foil optics – reflective optics – grazing incidence optics – x-ray optics – technology aspects

1. Introduction

Lobster eye (LE) optics (Schmidt, 1975; Angel, 1979) are a very promising technology for space X-ray sky monitors since the field of view can be orders of magnitude larger than other geometries of grazing incidence optics. LE optics are part of the payload of the VZLUSAT-1 mission (Baca et al., 2016; Pina et al., 2015) and they are considered as possible candidate in several other missions (Petre et al., 2015; Gorenstein, 2011; Fraser et al., 2002; Tichý et al., 2015). Apart from space astrophysics applications LE are also used in laboratory applications such as neutron imaging (Šaroun & Kulda, 2006).

This paper in particular deals with Schmidt lobster eye (SLE) (Schmidt, 1975). A one-dimensional SLE is composed of one stack of flat rectangular mirrors (Fig. 1). These mirrors form a uniform pattern around a virtual cylinder. Two such stacks can be arranged to form a two-dimensional SLE.

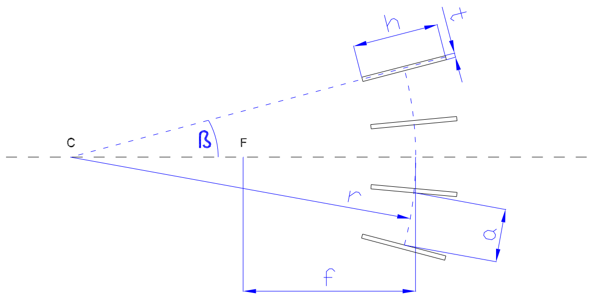

Figure 1. Lobster eye geometrical parameters.

A supporting structure is necessary to hold the mirrors in the SLE stack. Inaccuracies in the fabrication of the supporting structure and lack of flatness in actual mirrors introduce deviations from the ideal case (Tichý et al., 2011, 2009a,b). In this paper we investigate both aspects and how they affect the spatial resolution of SLE.

2. Experimental specimen LTW-51

To compare theory with experimental results, prototype lobster eye LTW-51 has been assembled, see Fig. 2. The prototype is one-dimensional, its focal length marked as f in Fig. 1 equals 51 cm. It is composed of 30 glass substrate mirrors of dimensions 37×37 cm, glass thickness t equals 0.28 mm. The pitch between centres of surfaces a is 0.995 mm. Mirrors are coated on both sides, so that the optic can operate in wide field mode. The coating consists of a bottom layer of gold and a 5 nm thin top layer of nickel. The coating has been made by TTS s.r.o., Prague, Czech Republic. The maximum grazing angle β is equal to 19.1 mrad $= 1.09°$.

The mirror plates are float-glass which has an observable ripple in one direction. This direction was aligned to lateral axis to minimize gradient errors at grazing incidence. At grazing incidence, mirror deformations in lateral axis are less significant because they cause only small shift of the reflection. Mirror deformations in optical axis cause change of reflection angle and therefore they have significant impact on image quality.

Figure 2. Schmidt lobster eye prototype LTW-51.

3. Glass profile measurements

Profiles of the mirror plates were measured by Fizeau interferometer, see Fig. 3. Mirrors were placed vertically and they were held by a special holder, see Fig. 4. Mirrors are held at corners marked by arrows and four mirrors can be accommodated in the holder.

The internal structure of the holder and a mirror itself is seen in Fig. 3. Because there is a small space around mirrors and there is a small space between mirrors and top part of the holder, the holder itself does not introduce a force on mirrors.

Typical profiles are shown in Fig. 6, Fig. 7. The profiles are of the same mirror but in Fig. 7, the mirror is physically rotated by 90° with respect to Fig. 6. Therefore, the difference between the profiles in figures Fig. 6, Fig. 7 are due to the effect of gravity.

4. Result of simulations for ideally assembled optics of ideally flat mirrors

First, the simulations of LTW-1 were performed with the assumptions that mirrors are idealy flat and ideally assembled. The simulations were performed via software package QSOFT developed at University of Leicester. This and all other presented simulations were performed for aligned optics with on-axis

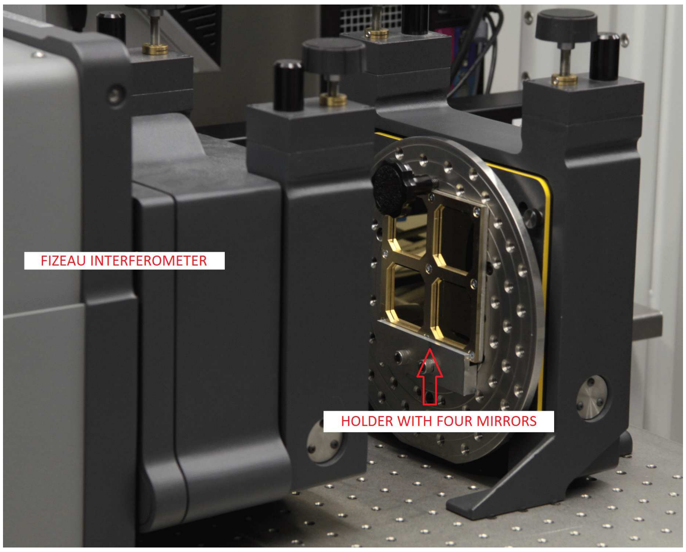

Figure 3. Setup for mirror profiles measurement using the Fizeau interferometer.

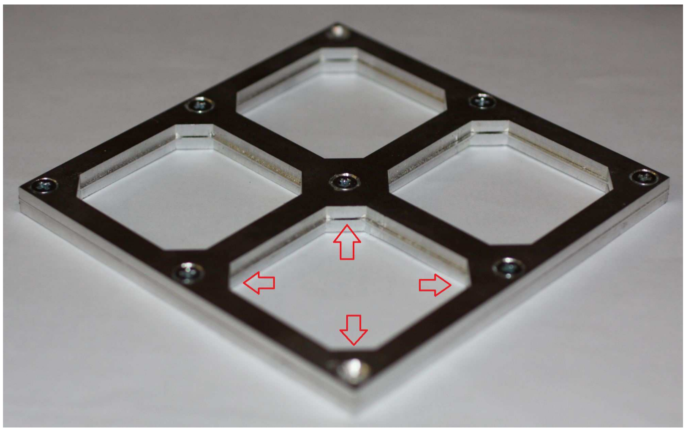

Figure 4. Holder for mirrors profile measurement.

source. As model of reflectivity, a look-up table of data acquired at Henke (2017) were used. The same incident energy of 1490 eV was used in the simulations and in the experiment.

The resulting simulated image for a perfect optic is shown in Fig. 8. The FWHM of the line focus equals 0.4 mm. This and all FWHM values in this paper were estimated as average of result of five simulations made with resolution

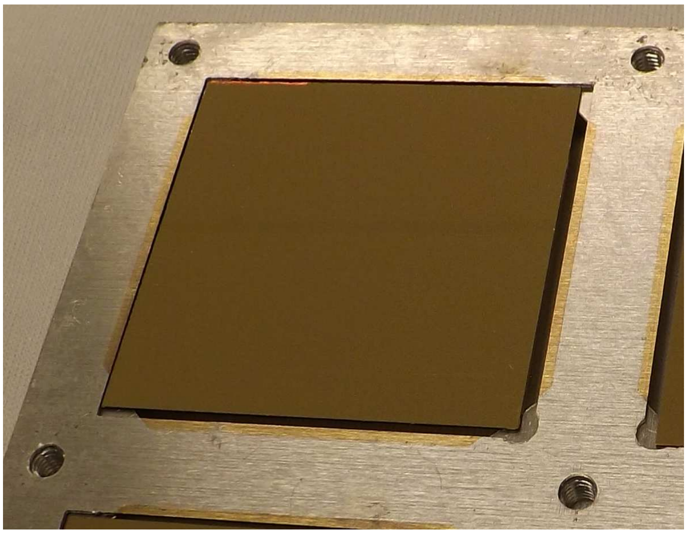

Figure 5. Mirror and holder internal structure detail.

of 0.1 mm. The average was rounded to tenths of mm. The image in Fig. 8 represents a typical image acquired by one-dimensional SLE for parallel incoming beam. The bright central line represents the line focus. It is formed by single reflections. Fainter lines laying beside the central line are formed by unreflected rays that come through the SLE directly. The outer strips are unreflected rays that penetrate between the outer plates and the housing.

5. Simulation of mirror intrinsic deformations

Measured mirror intrinsic deformations are irregular and differ from mirror to mirror. Usually, profile data were not acquired over the entire mirror area. For this reason, measured data cannot be directly used for modelling of mirror intrinsic deformations.

However, it was found that intrinsic mirror deformation in worse axis has wavelengths of around 20 mm and amplitudes (peak to peak) around 1 μm as seen in the Fizeau data. As a first approximation, a sine wave was chosen to model the deformation in one axis. I.e. the function $\delta = A\sin(x/\lambda - \phi)$ was used as a model of the deformation. A Gaussian distribution of mean value 0.5 μm and $\sigma = 0.125$ nm was used for random generation of amplitude A. For period λ, Gaussian distribution of mean value 20 mm and $\sigma = 5$ mm was used. For generating of phase ω, uniform distribution on interval $[0, 2\pi)$ was used. These numbers were individually generated for each mirror.

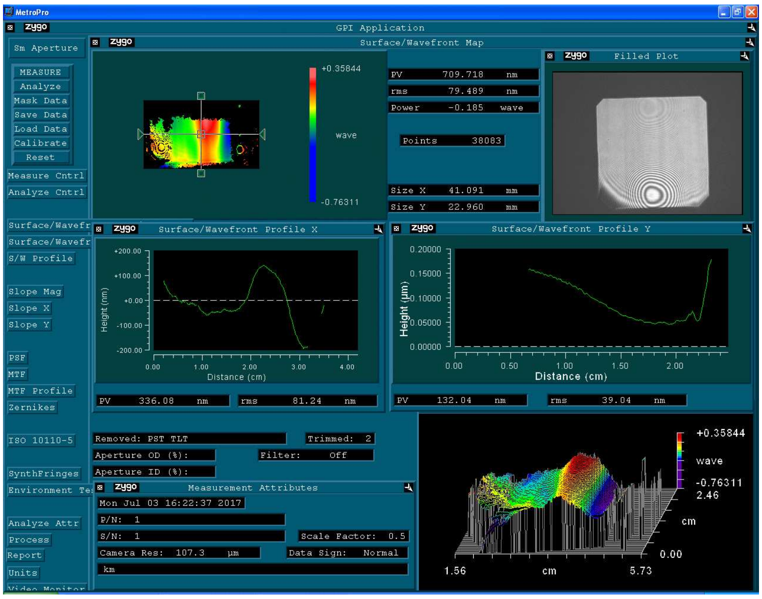

Figure 6. Typical mirror profiles. In the left-hand middle panel, there is the lateral profile. In the right-hand middle pannel, there is the optical axis profile.

If the deformations are placed along the lateral axis, the deflections are so small and not seen in the result of simulations and the FWHM is unchanged. If the deformations are placed along the optical axis, FWHM increases to 0.6 mm. The resulting image is shown in Fig. 9.

6. Simulation of mirror positioning errors

Four randomly generated numbers were used to represent shifts in the corners of the mirrors. These shifts were individually generated for each mirror. They were added to values representing ideal positions of corners. Between the corners, linear interpolation was used to represent the profile of mirrors. This approach simulates first order mirror deformations that can be caused by the mirror supporting structure. A Gaussian distribution with various values of σ and zero mean was used. Results are shown in Fig. 10. Deviations in mirror positioning introduce tilt errors in the mirrors which cause a blurring of the line focus.

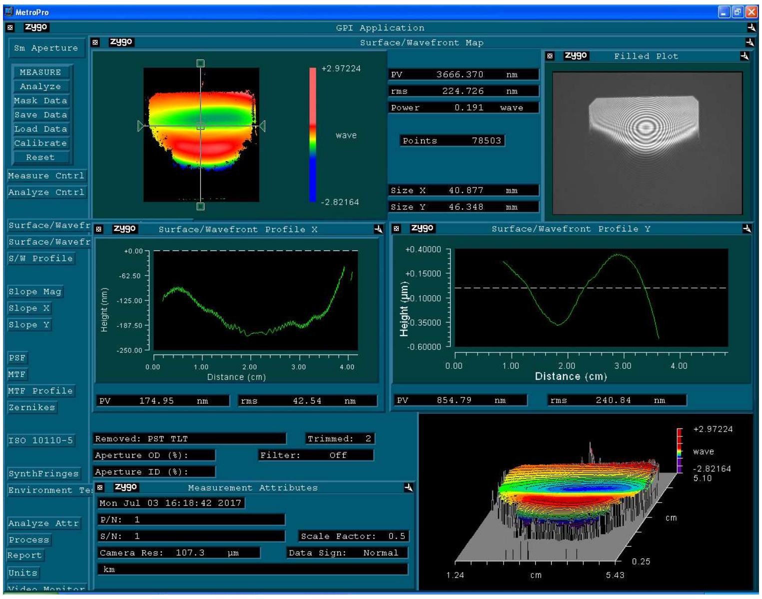

Figure 7. Typical mirror profiles. In the left-hand middle pannel, there is the optical axis profile. In the right-hand middle pannel, there is the lateral profile.

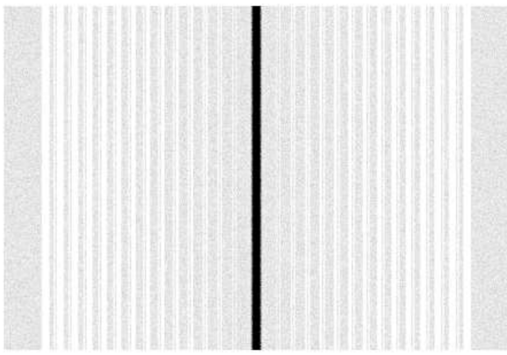

Figure 8. Results of simulation for ideally assembled SLE with ideally flat mirrors.

7. Experimental results with LTW-51

The Prototype lobster eye LTW-51 was tested at the XACT facility (Artale et al., 2004; Barbera et al., 2006) in the 35 m long X-ray beam-line. X-ray image at the focal plane has been taken with a microchannel plate (MCP) detector

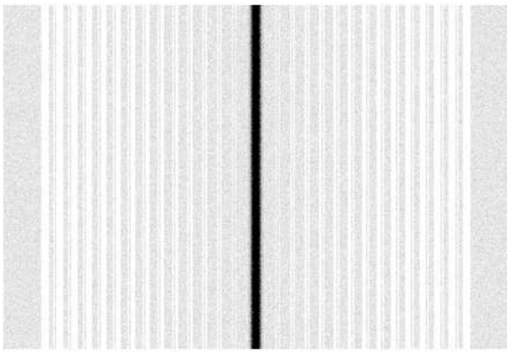

Figure 9. Results of simulation for ideally assembled SLE with mirrors including deformations in the optical axis.

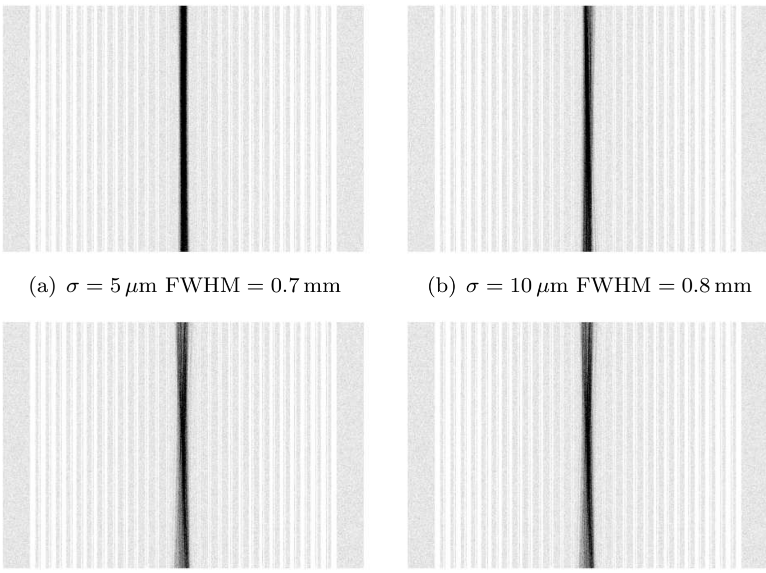

(a) $\sigma = 5\,\mu$m FWHM = 0.7 mm
(b) $\sigma = 10\,\mu$m FWHM = 0.8 mm
(c) $\sigma = 15\,\mu$m FWHM = 1.0 mm
(d) $\sigma = 20\,\mu$m FWHM = 1.3 mm

Figure 10. Simulation of deviations of supporting structure.

featuring a $100\,\mu$m spatial resolution at energy 1490 eV. The setup in the test chamber is shown in Fig. 11.

The image acquired at centered, on-axis position is shown in Fig. 12(a) FWHM reaches 0.7 mm. This value of FWHM was obtained in simulations us-

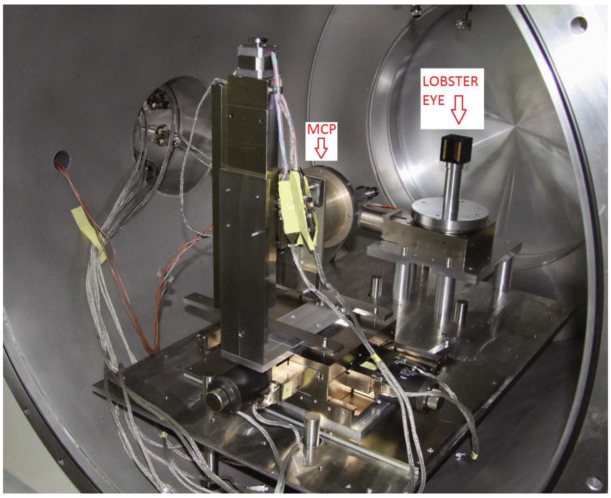

Figure 11. Test chamber setup.

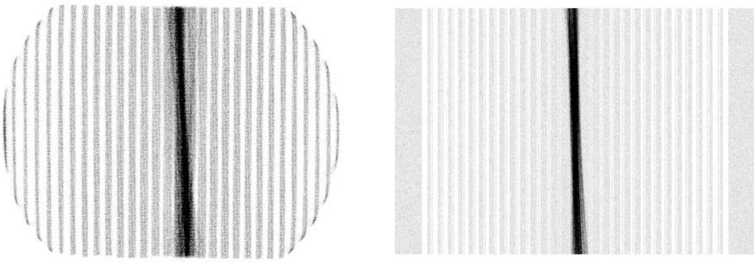

(a) Experimental image.

(b) Simulation including skew error $10\,\mu$m and mirror positioning error $\sigma = 5\,\mu$m.

Figure 12. Final results.

ing a positioning error of $\sigma = 5\,\mu$m. The small skew is caused by position shift between opposite parts of supporting structure and it was estimated as $10\,\mu$m. This skew was simulated as systematic shift of mirror corner points. The above values were used for the final simulation with the skew and supporting structure inaccuracy included. The result is shown in Fig. 12(b).

8. Conclusions

The principal manufacturing errors of Schmidt lobster eye have been described and simulated.

For a size of 51 cm focal length, 37 mm mirror size and ca. 1 mm mirror pitch, the results indicate that the critical task is to place mirrors into their ideal positions. To achieve the theoretically possible angular resolution, micron or submicron accuracy are necessary.

The glass employed shows significantly different deformations in different axes. The current results indicate that glass deformations are less significant or they are not significant if they are aligned laterally.

Acknowledgements. For the financial support, we thank to AHEAD (Integrated Activities in the High Energy Astrophysics Domain) project funded by the European Union as Research and Innovation Action under Grant No: 654215.

We would like to thank the Grant Agency of the Czech Republic for the financial support by grant number 13-33324S.

Authors would like to thank INAF-Osservatorio Astronomico di Palermo for providing the use of the X-ray beam-line for the experiment.

References

Angel, J. R. P., Lobster eyes as X-ray telescopes. 1979, *Astrophys. J.*, **233**, 364, DOI: 10.1086/157397

Artale, M. A., Barbera, M., Collura, A., et al., Calibration of the XRT-SOLARB flat mirror samples at the XACT Facility of INAF-OAPA. 2004, in Proc. SPIE, Vol. **5488**, *UV and Gamma-Ray Space Telescope Systems*, ed. G. Hasinger & M. J. L. Turner, 440–448

Baca, T., Platkevic, M., Jakubek, J., et al., Miniaturized X-ray telescope for VZLUSAT-1 nanosatellite with Timepix detector. 2016, *Journal of Instrumentation*, **11**, C10007, DOI: 10.1088/1748-0221/11/10/C10007

Barbera, M., Candia, R., Collura, A., et al., The Palermo XACT facility: a new 35 m long soft x-ray beam-line for the development and calibration of next-generation x-ray observatories. 2006, in Proc. SPIE, Vol. **6266**, *Society of Photo-Optical Instrumentation Engineers (SPIE) Conference Series*, 62663F

Fraser, G. W., Brunton, A. N., Bannister, N. P., et al., LOBSTER-ISS: an imaging x-ray all-sky monitor for the International Space Station. 2002, in Proc. SPIE, Vol. **4497**, *X-Ray and Gamma-Ray Instrumentation for Astronomy XII*, ed. K. A. Flanagan & O. H. W. Siegmund, 115–126

Gorenstein, P., Large-angle observatory with energy resolution for synoptic x-ray studies (LOBSTER-SXS). 2011, in Proc. SPIE, Vol. **8147**, *Society of Photo-Optical Instrumentation Engineers (SPIE) Conference Series*, 81471O

Henke. 2017, http://henke.lbl.gov/optical_constants/

Petre, R., Camp, J., Barthelmy, S., et al., ISS-Lobster: a low-cost wide-field X-ray transient detector on the ISS. 2015, in *APS Meeting Abstracts*

Pina, L., Hudec, R., Inneman, A., et al., X-ray monitoring for astrophysical applications on Cubesat. 2015, in Proc. SPIE, Vol. **9510**, *EUV and X-ray Optics: Synergy between Laboratory and Space IV*, 951005

Schmidt, W. K. H., A proposed X-ray focusing device with wide field of view for use in X-ray astronomy. 1975, *Nuclear Instruments and Methods*, **127**, 285, DOI: 10.1016/0029-554X(75)90501-7

Tichý, V., Barbera, M., Collura, A., et al., Tests of lobster eye optics for small space X-ray telescope. 2011, *Nuclear Instruments and Methods in Physics Research A*, **633**, S169, DOI: 10.1016/j.nima.2010.06.157

Tichý, V., Burrows, D. N., Prieskorn, Z., & Hudec, R., Optics for nano-satellite X-ray monitor. 2015, *Baltic Astronomy*, **24**, 243

Tichý, V., Hromčík, M., Hudec, R., et al., Small x-ray telescope based on lobster eye x-ray optics and pixel detector. 2009a, in Proc. SPIE, Vol. **7360**, *EUV and X-Ray Optics: Synergy between Laboratory and Space*, 736011

Tichý, V., Hromčík, M., Hudec, R., et al., Tests of Lobster-Eye Optics for a Small X-Ray Telescope. 2009b, *Baltic Astronomy*, **18**, 362

Šaroun, J. & Kulda, J., MC ray-tracing optimization of lobster-eye focusing devices with RESTRAX. 2006, *Physica B Condensed Matter*, **385**, 1250, DOI: 10.1016/j.physb.2006.06.022